Assessing simulated visible greenness in urban environments

Jingjing Yan[1[0000−0002−4582−5490]] and Xiao Huang[1,2[0000−0002−4323−382X]]

[1] University of Arkansas, Fayetteville AR 72701, USA
{jy016, xh010}@uark.edu
[2] Emory University, Atlanta GA 30322, USA
xiao.huang2@emory.edu

Abstract. Urban greenness is critical in evaluating the urban environment and living conditions, significantly affecting human well-being and house prices. Unfortunately, satellite imagery from a bird-eye view does not fully capture urban greenness from a human-centered perspective, while human-perceived greenness from street-view images heavily relies on road networks and vehicle accessibility. In recent years, scholars started to explore greenness measurements from a simulative perspective, among which the simulation of the Viewshed Greenness Visibility Index (VGVI) received wide attention. However, the simulated VGVI lacks a comprehensive assessment. To fill this gap, we designed a field experiment in Fayetteville, Arkansas, by collecting 360-degree panoramas in different local climate zones. Further, we segmented these panoramas via the state-of-the-art DeeplabV2 neural network to obtain the Panoramic Greenness Visibility Index (PGVI), which served as the ground-truthing hu-man-perceived greenness. We assessed the performance of VGVI by comparing it with PGVI calculated from field-collected panoramas. The results showed that, despite the disparity of performance in different local climate zones, VGVI significantly correlates to the PGVI, indicating its great potential for various domains that favor urban human-perceived greenness exposure.

Keywords: Visible greenness · 360-degree panoramas · DeeplabV2 neural network.

DOI: https://doi.org/10.25436/E2GW2W

1 Introduction

The rapid growth of the urban population accelerated the expansion of the urban and metropolitan areas, leading to a big challenge for urban planning and management, especially for the maintenance and development of greenspace [11]. Urban greenness (i.e., vegetation) is an essential criterion for evaluating the living environment in various aspects of human health. Satellite imagery brings an overview of the spatial distribution of green and non-green space, which can help

estimate the macroscopical environmental effect of urban greenness, however, it cannot provide detailed guidance for assessing housing prices or human health enhancement because it fails to reflect the greenness from a human-eye aspect [3]. How to de-rive visible greenness from the human eye has become a hot research topic.

With the development of street view images, recent studies proposed a photo-based urban greenness assessment from a profile view by extracting the greenness level from street view images [10]. However, photo-based urban greenness is only accessible where street-view vehicles are reachable [7]. Simulated urban greenness, a geospatial data-based method to calculate greenness, can overcome such challenges. A new integrated simulation of VGVI is developed to assess urban greenness [10], which gained wide attention. In the simulation of VGVI, not only the viewshed analysis was applied, but a distant decay function was also incorporated to simulate the effect of the human eye perceptron discrepancy within various distances. The concept of VGVI is displayed in Fig. 1. From the reader's perspective, a sizeable green area can be observed, while only green belts (i.e., the grass and trees) on both sides of the road are visible to the observer standing at the pedestrian crossing.

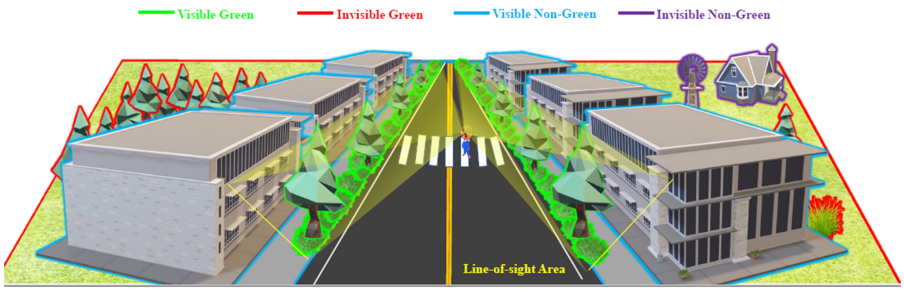

Fig. 1. Conceptual display of Viewshed Greenness Visibility Index (VGVI).

However, the lack of comprehensive evaluation of the simulated urban greenness hinders its applications, especially the assessment in different urban settings. In this study, we aim to conduct a comprehensive evaluation of the VGVI and investigate its adaptation under different Local Climate Zones (LCZs) which was proposed by Demuzere et al. [7]. LCZs reflect the association between urban land cover and land use and are a widespread new category of urban environ-

ments. To achieve these objectives, we applied the VGVI to our study site, i.e., Fayetteville, Arkansas, which is a typical mid-size city in the United States of America (U.S.). We collected panoramas within complex urban settings to derive a panoramic greenness visibility index (PGVI) and further used the PGVI as the ground truth to evaluate the performance of VGVI.

2 Methods and Materials

2.1 Experimental design

To assess the performance of VGVI, we designed a field experiment to collect the 360-degree panoramas and further compute the Panoramic Greenness Visibility Index (PGVI) from these panoramas, especially for those locations that are not vehicle-accessible. The sample collecting date happened in the green season of Fayetteville, mainly in the summer of 2022. The PGVI served as the ground-truthing eye-level greenness in Fayetteville under different LCZs. In Fayetteville, there are a total of 8 LCZs are involved in this study, including five built types (i.e., compact lowrise, open midrise, open lowrise, large lowrise, and sparsely built) and five natural land cover types (i.e., dense trees, scattered trees, low plants). Corresponding with the original LCZ index, the five built types of compact lowrise, open midrise, open lowrise, large lowrise, and sparsely built are named LCZ 3, 5, 6, 8, and 9, respectively. The dense trees, scattered trees, and low plants correspond to LCZ 11, 12, 14, 16, and 17, respectively. Fig. 2 presents the workflow of our experiment.

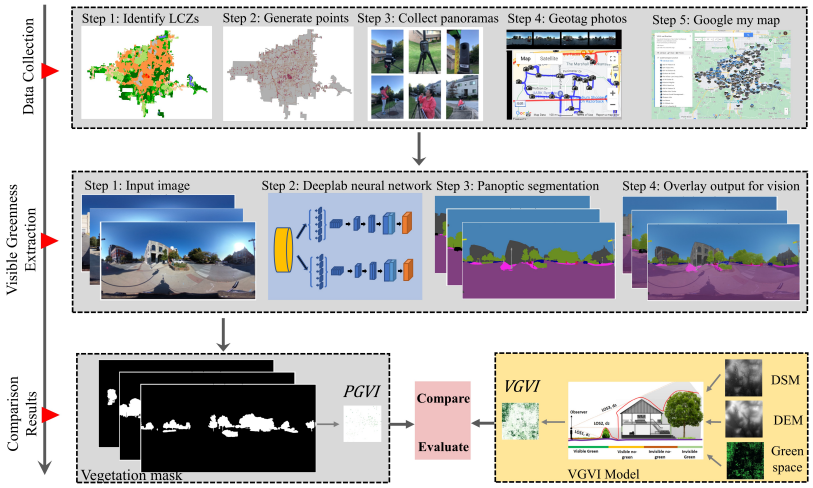

Fig. 2. Experimental workflow of this study.

Sampling protocols (1) Identifying the area for each type of LCZ in Fayetteville (a total of eight LCZ types); (2) Creating 100 random sampling points along the street for each LCZ (a total of 800 locations); (3) Collecting panorama for each random pointed location or its near location for convenience and safety; (4) Geotagging the panoramas and importing them to Google MyMap for documentation (shorturl.at/LRV29). When we tried to collect the samples in other LCZs, some samples were not easily reachable, so we chose a nearby location to collect the data for convenience. Thus, several samples from other LCZs fell into the other LCZ. Finally, a total of 858 panoramas were obtained in our experiment.

Calculation of PGVI from greenness segmentation We applied a pre-trained DeepLab2 model to extract the urban greenness from the panoramas. This pre-trained model was trained on the Cityscapes datasets [6] through the Wide-ResNet-41 backbone in Panoptic-DeepLab segmentation [4]. After obtaining the pixel-based feature map, the non-vegetation category in the semantic labels was removed, and PVGI can be calculated as follows:
Displayed equations are centered and set on a separate line.

$$PVGI_{deeplab2} = \frac{NoP_{veg}}{NoP_{total}} \tag{1}$$

where NoP_{veg} is the number of vegetation pixels and the NoP_{total} is the total number of pixels in the panoramas.

2.2 VGVI Calculation

To set the eye-level view aspect, we considered a modified observer height of 1.7m at a given location to launch the LOS and set the maximum view distance as 550m based on the method from Labib et al. [9]. DSM and DEM are derived from LiDAR and provided by the US Geological Survey [8]. Following the early study [2], we calculated green and non-green spaces from high-resolution normalized difference vegetation index (NDVI) derived from the National Agriculture Imagery Program (NAIP) in the growing season of 2022.

According to Labib et al., [9], viewshed analysis and distant decay served as the main component parts of VGVI modeling. For any given observer spot, a matrix of visibilities that depicts visible information is generated through the viewshed analysis, and a matrix of weights is generated through the distant decay function. The products of these two matrixes of visibilities and weights contribute to the VGVI. The mathematical formation of VGVI follows:

$$VGVI_j = \frac{\sum_{p=1}^{n} G_{pj} \times df_{pj}}{\left(\sum_{p=1}^{n} G_{pj} \times df_{pj}\right) + \left(\sum_{q=1}^{m} V_{qj} \times df_{qj}\right)} \tag{2}$$

where $VGVI_j$ is the greenness visible index value at any observer location j; p represents the pth visible green cell for the observer location; q represents the qth

visible non-green cell for the observer location; n and m, respectively, represent the total number of visible green and non-green cells. G_pj is the pth visible green cell, V_qj is the qth visible non-green cell, and df_pj stands for the pre-calculated weights by distance decay function at the pth visible green cell for observer location j. Similarly, df_qj represents the weights at the qth visible non-green cell. Thus, the VGVI, ranging from 0 to 1, represents the proportion of the visible green cells over the total visible cells.

2.3 Evaluation of VGVI

In this study, we compare the correlation between field-collected PGVI and simulated VGVI, aiming to shed light on the performance of VGVI. A 95% significance level was selected for statistical tests.

3 Results

3.1 Greenness segmentation from panoramas

Fig 3 presents the PGVI calculated from the greenness extraction with different green tones of dots. The average PGVI for all the sampling points is 0.13, meaning the average greenness derived from the panoramas is 13%. The area with more dense buildings, such as the downtown and the University of Arkansas, exhibits a lighter green tone than the suburban area, indicating their lower visible greenness. The building acts as a major factor that obstructs sight [1]. The histograms in Fig. 3 show the distribution of PGVI in each LCZ. In general, LCZ 11 (i.e., dense tree), shows a relatively higher greenness level with an average PGVI of 0.293, and LCZ 14 (i.e., low plants), shows a lower greenness level with an average PGVI of 0.058. For the built types (i.e., LCZ3-9), the PGVI is around 0.1.

3.2 VGVI distribution

In our study area, we simulate VGVI in more than 235 million observing locations, using high-performance computers and R programming running on the Linux operating system. Fig 4 shows the spatial distribution of VGVI in the study area. The average value of VGVI for the whole city is 0.49, with a standard deviation of 0.36. The average value reveals that nearly 50% of greenness visibility appears in Fayetteville, and this percentage is close to the rate of forestland (56%) in Arkansas [5]. We also observe that the spatial distribution of VGVI is uneven and heterogeneous. Typically, the highest values occur in parks and natural areas, such as Centennial Park, Kessler Park, and Wilson Springs Nature Preserve. Despite the high greenness visibility in the forest, those areas are hard-to-access places for citizens. Low VGVI values occur in the downtown areas, suggesting low greenness visibility in these areas.

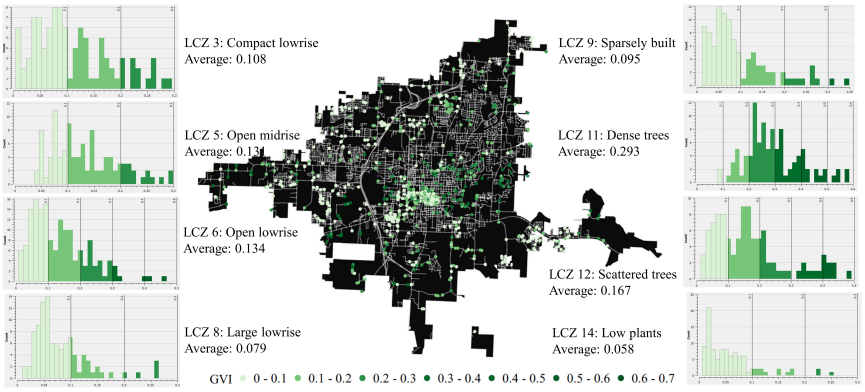

Fig. 3. The PGVI distribution from collected panoramas in our study area via Deeplabv2 segmentation. In the histograms, the x-axis denotes PVGI, and the y-axis denotes the count of samples.

Figure 7. (a) VGVI distribution; (b) Greenspace distribution

Fig. 4. The distribution of VGVI (eye-level view) in Fayetteville.

3.3 The correlation between simulated VGVI and panoramic greenness

The correlation between VGVI and ground-truthing PGVI from the collected panoramas is presented in Fig 5. A significant positive correlation (0.5) is observed for all the sampling cases, suggesting the robustness of VGVI in simulating visible greenness in complex urban settings. When evaluating the results at the LCZ level, we notice that all the LCZs show a significant positive correlation between the VGVI and PGVI, except for the LCZ 3 (i.e., compact lowrise) and LCZ 14 (i.e., low plants). Moreover, based on the marginal density curves, the VGVI demonstrates that the visible greenness in the area of natural land cover types (i.e., LCZ 11-14) is typically higher than the greenness in the area of built types (i.e., LCZ 3-9). This result is consistent with ground-truthing PGVI, which also partially demonstrates the robustness of the VGVI.

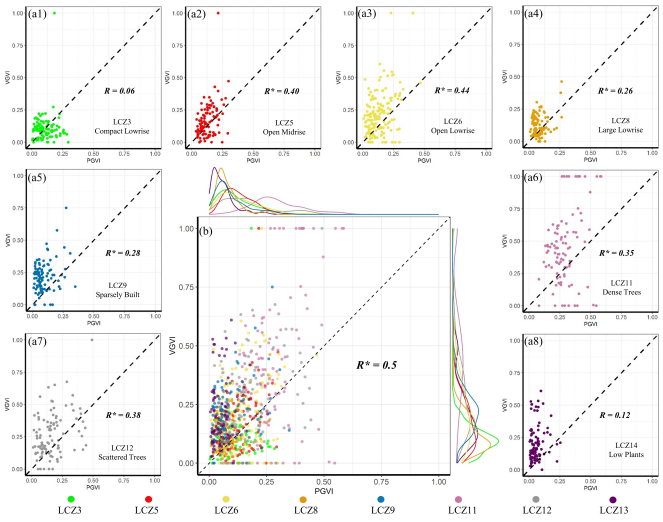

Fig. 5. (a1) - (a8) Scatter plots of simulated VGVI and field-collected PGVI from each LCZ. (b) Scatter plot for all samples from eight LCZs with their marginal density plots, and the dots are with 70% transparency for a better view. R means the correlation coefficient of VGVI and PGVI, and the R with * represents significance at the 0.01 significance level.

Regarding the insignificant results in LCZ3, the existence of dense buildings can partly explain the insignificant correlation in LCZ 3, as dense buildings pose challenges in extracting VGVI at some sampling points. These points might be close to the facilities or objects like cars that existed when the aircraft with sensors collected the LiDAR point cloud dataset but did not exist when the panoramas were taken. Another potential reason is the sensitivity of resolution

in LCZ 3, where dense buildings are widely distributed. A small error in line-of-site can be translated to a large variation of VGVI. In addition, for LCZ 14 (represented by the light green color in Fig. 5, we notice that the VGVI is higher than the PGVI. We believe the grass greenness extraction from panoramas is the leading cause of the mismatch between VGVI and PGVI within LCZ 14 (low plants). Despite the mismatches in these two LCZs, we still believe the VGVI from a 3D urban environment is largely consistent with the PGVI collected from panoramas.

4 Discussion

Most existing greenness availability or accessibility studies, however, rely on bird-eye greenness distribution, largely detaching from human experience. In this study, we implemented the VGVI model that simulated visible greenness under a 3D urban context and investigated the performance of VGVI using field-collected panoramas. The results pointed to the promising aspects of visible greenness simulation, as the simulated results present a high consistency compared with ground observations. As Fayetteville, our experimental site, belongs to a mid-size U.S. city, we assume such inconsistency is likely to be exaggerated in bigger cities with denser buildings. We consider simulated visible greenness a promising measure for various domains that favor urban human-perceived greenness exposure, such as environmental psychology, public health (especially mental health), and urban aesthetics.

Despite the promising future of visible greenness simulation, several challenges deserve to be mentioned. We notice that such simulation is computationally intensive and demands high-performance computer infrastructure. Even with the support of high-performance computers, obtaining the distribution of simulated visible greenness in this mid-size U.S. city still takes hours. The computational demand is expected to increase exponentially for larger geographic areas. We encourage more efforts toward designing a parallel-computing-enabled simulation environment. In addition, urban environments are dynamic, with fast changes in landscapes, posing additional demand for temporal regularity of the input datasets. Three input datasets are required for the VGVI model, i.e., DEM, DSM, and bird-eye greenness. Ideally, these three datasets need to be collected at the same or close temporal frames to ensure an accurate simulation of visible greenness. Nonetheless, such coordination of the datasets mentioned above is rare, especially with the demand for high-resolution ones

5 Conclusion

In this study, we demonstrated the robustness and usefulness of the simulated greenness (VGVI) to quantify human eye-level visible greenness by comparing it with the ground-truthing panoramic greenness (PVGI) derived from the panoramas. This study marks the first effort to comprehensively evaluate the robustness

of the simulated greenness, providing a solid and scientific basis for future large-scale and even national-wide investigations. Specifically, our results pointed to a significant correlation that passes the 0.01 significance level between the simulated greenness VGVI and PVGI. When evaluating the results at the LCZ level, we noticed that most LCZs show a significant positive correlation between the simulated greenness VGVI and PVGI from field-collected panoramas. Despite the disparity of performance in different LCZs, we believe VGVI is a promising measure for various domains that favor urban human-perceived greenness exposure, such as environmental psychology, public health (especially mental health), and urban aesthetics. Considering its advantage in obtaining human-perceived greenness in any location in urban areas (not restricted by the availability of street view images), we encourage more efforts to explore the potential of VGVI in various applications of urban green spaces.

References

1. Biljecki, F., Ito, K.: Street view imagery in urban analytics and gis: A review. Landscape and Urban Planning **215**, 104217 (2021)
2. Braun, M., Herold, M.: Mapping imperviousness using ndvi and linear spectral unmixing of aster data in the cologne-bonn region (germany). In: remote sensing for environmental monitoring, gis applications, and geology iii. vol. 5239, pp. 274–284. SPIE (2004)
3. Chen, X., Meng, Q., Hu, D., Zhang, L., Yang, J.: Evaluating greenery around streets using baidu panoramic street view images and the panoramic green view index. forests 10 (12), 1109 (2019)
4. Cheng, B., Collins, M.D., Zhu, Y., Liu, T., Huang, T.S., Adam, H., Chen, L.C.: Panoptic-deeplab: A simple, strong, and fast baseline for bottom-up panoptic segmentation. In: Proceedings of the IEEE/CVF conference on computer vision and pattern recognition. pp. 12475–12485 (2020)
5. Chhetri, S.G., Pelkki, M.: Current forest management intensity and cost associated with major forestry practices in arkansas, usa. Journal of Forest Business Research **1**(1), 51–74 (2022)
6. Cordts, M., Omran, M., Ramos, S., Rehfeld, T., Enzweiler, M., Benenson, R., Franke, U., Roth, S., Schiele, B.: The cityscapes dataset for semantic urban scene understanding. In: Proceedings of the IEEE conference on computer vision and pattern recognition. pp. 3213–3223 (2016)
7. Demuzere, M., Kittner, J., Martilli, A., Mills, G., Moede, C., Stewart, I.D., van Vliet, J., Bechtel, B.: A global map of local climate zones to support earth system modelling and urban scale environmental science. Earth System Science Data Discussions **2022**, 1–57 (2022)
8. Dollision, R., Maxwell, J.: The national map—new data delivery homepage, advanced viewer, lidar visualization. fact sheet.(2019)
9. Labib, S., Huck, J.J., Lindley, S.: Modelling and mapping eye-level greenness visibility exposure using multi-source data at high spatial resolutions. Science of the Total Environment **755**, 143050 (2021)
10. Li, X., Zhang, C., Li, W., Ricard, R., Meng, Q., Zhang, W.: Assessing street-level urban greenery using google street view and a modified green view index. Urban Forestry & Urban Greening **14**(3), 675–685 (2015)

11. Muhamad Nor, A.N., Abdul Aziz, H., Nawawi, S.A., Muhammad Jamil, R., Abas, M.A., Hambali, K.A., Yusoff, A.H., Ibrahim, N., Rafaai, N.H., Corstanje, R., et al.: Evolution of green space under rapid urban expansion in southeast asian cities. Sustainability **13**(21), 12024 (2021)